2016 IEEE/RSJ International Conference on Intelligent Robots and Systems (IROS)
Daejeon Convention Center
October 9-14, 2016, Daejeon, Korea

Vision-based Precision Manipulation with Underactuated Hands: Simple and Effective Solutions for Dexterity

Berk Calli, *Member IEEE*, Aaron M. Dollar, *Senior Member, IEEE*

***Abstract*— In this paper, a method is proposed for vision-based within-hand precision manipulation with underactuated grippers. The method combines the advantages of adaptive underactuation with the robustness of visual servoing algorithms by employing simple action sets in actuator space, called precision manipulation primitives (PMPs). It is shown that, with this approach, reliable precision manipulation is possible even without joint and force sensors by using only minimal gripper kinematics information. An adaptation method is also utilized in the vision loop to enhance the system's transient performance. The proposed methods are analyzed with experiments using various target objects and reference signals. The results indicate that underactuated hands, even with minimalistic sensing and control via visual servoing, can provide a simple and inexpensive solution to allow low-fidelity precision manipulation.**

I. Introduction

Gripper dexterity brings flexibility to robotic object manipulation: Besides enriching the possibilities for object grasping, dexterity reduces task specific dependencies on initial grasp configuration by enabling precision (within-hand) object manipulation. Such properties are especially important for home/service robots, which are expected to manipulate daily-life objects that are designed for dexterous human hand. In addition, gripper dexterity, and in particular precision fingertip-based manipulation, helps to avoid joint limits of the robot and increases energy efficiency of the system by obviating the need for larger arm motions [1], [2].

Assuming that the gripper model, object model, and contact locations are accurately known and joint states can be measured, precision manipulation can be implemented by utilizing the models in [3]–[7]. These models calculate gripper actuator positions for a given desired object pose, along with conditions to satisfy force balance in quasi-static cases given a contact model. Nonholonomic motions of the object within hand (such as sliding) are neglected. Unfortunately these assumptions are far from being realistic in unstructured environments in which object models are usually unknown a priori, nonholonomic motions are common and assumptions on contact models may not exactly hold in practice. Combination of these modeling errors results in significant steady state error or even dropping the target object.

Using vision feedback is a natural solution to some of the aforementioned problems. Robustness to modeling

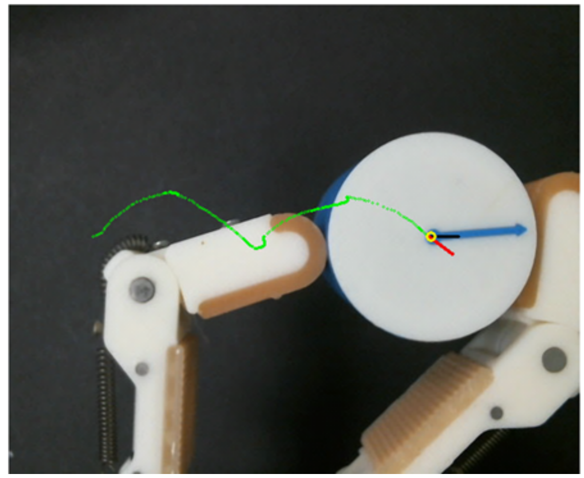

Figure 1. Precision manipulation via vision feedback using an underactuated hand: Controlling the position of the object center for following a trajectory in the image space.

inaccuracies can be achieved by taking inherent advantages of some visual servoing methods. Even though vision-based precision manipulation methods are presented in literature for fully-actuated grippers, no methods are proposed for underactuated grippers.

In this work we examine vision-based precision manipulation with underactuated grippers (Fig. 1). Using vision feedback and minimal information about the underactuated mechanism, we achieved accurate positioning while maintaining a stable grasp without the use of any joint encoders or force sensors. This success is due to combining the robustness of visual servoing methods with the contact stability provided by adaptive underactuation via *precision manipulation primitives (PMPs)*. It was observed that the proposed simple architecture is robust to contact position changes and nonholonomic motions of the object within hand. For improving the system's transient response, an adaptive method was also employed. Apart from being the first work that focuses on visual servoing techniques applied to underactuated hands, the novelty of the paper also lies in our proposed methodology that uses manipulation primitives for vision-based precision manipulation. Moreover, unlike many previous works, which provide limited experimental evaluation, we present extensive set of experiments for performance analysis.

In the next section, we summarize the literature on precision manipulation and its vision-based implementations. In Section III our proposed method is explained. Following that, Section IV provides experimental results, and Section V concludes the paper with discussions.

Research supported by U.S. National Science Foundation under the grant IIS-1317976.

B. Calli and A. M. Dollar are with the Dep. of Mech. Eng. and Mater. Science, Yale University, CT, USA ({berk.calli;aaron.dollar}@yale.edu).

II. RELATED WORK

In this section, the literature on precision manipulation and the use of visual servoing algorithms in the field are summarized.

A. Underactuated Grippers and Precision Manipulation

Underactuated grippers are proved to be useful for many robotic grasping scenarios. With their unconstrained degrees of freedom which allow them to reconfigure, they adapt to the object shape, increase the contact with the object and maintain a stable grasp [8], [9]. In addition, due to the reduced number of actuators, underactuated architectures allow compact designs and provide cheap solutions.

It is also shown in literature that these grippers are capable of precision manipulation [10]–[13]. Nevertheless, additional design considerations are necessary to maintain a stable pinch grasp during the manipulation. In [11], stability of precision manipulation with underactuated hands are examined and it is concluded that there must be elastic elements, which provide a restoration force for any unconstraint motion of the hand-object couple. These forces should be large enough for the hand to deliver enough normal force to the object in order to avoid slipping and sliding. The required force can be reduced by using a higher friction finger surface.

Once the abovementioned design criteria are met, even open-loop precision manipulation is possible with underacted hands, since the mechanical restoration force will maintain the contact between the object and the finger without the need of any sophisticated control and planning algorithms (this property is essential for this paper and will be re-visited in Section III). This is, of course, valid only within the gripper's manipulation workspace, which is studied in [10], [11]; due to underactuation, the portion of the Cartesian workspace spanned by the gripper is limited to its degrees of freedom and actuator arrangements.

The precision manipulation strategies with underactuated grippers (i.e. [10]–[13]) often require an accurate knowledge of gripper model, object model and contact locations (an exception with unknown object models is given in [14] where a particular gripper morphology is needed). Using these information, precision manipulation can be analyzed by energy minimization methods [11] or by considering the hand-object system as a parallel robot [15]. Unfortunately, generating accurate models for underactuated grippers are difficult due to their elastic elements and friction. Moreover, in most precision manipulation scenarios, contact locations may not be accurately known or may change in time due to nonholonomic motions.

Even though vision feedback is utilized in order to tackle similar problems in precision manipulation with fully-actuated grippers, its use with underactuated grippers is not addressed in literature.

B. Visual Servoing and Precision Manipulation

Visual servoing is a well-established field with many applications in robotics [16]–[18]. Their applications are also proposed for precision manipulation with fully-actuated grippers [19]–[25]. Mainly, the three basic methods used in literature are Image-based Visual Servoing (IBVS), Position-based Visual Servoing (PBVS) and 2.5D Visual Servoing.

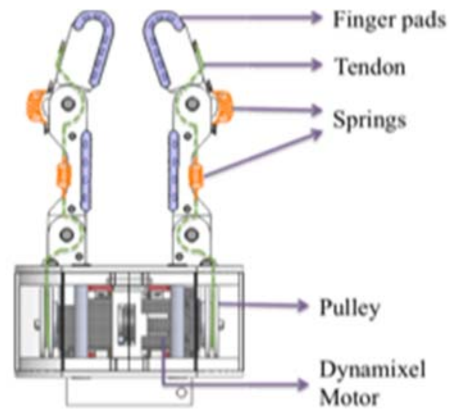

Figure 2. Model T42 hand.

In scenarios where the reference pose can be formulated in image space, IBVS and 2.5D Visual Servoing can be utilized. These methods generate velocity references to the system by using image features, and therefore, do not require object model to be known. Moreover, both of these techniques are robust to camera calibration and modeling errors (in our case the process model includes gripper model and contact locations), and they perform adequately under noisy conditions [26].

Alternatively, PBVS method can be used to control the position of the object in Cartesian space if the pose of the object can be determined. In this case, the system is vulnerable to camera calibration inaccuracies since they result in errors while calculating the object pose, and these errors are directly observed in steady state. However, PBVS is still robust to inaccuracies in gripper model and contact locations.

Essentially, these advantages provided by visual servoing algorithms are only valid if the contact between the gripper and the object can be preserved; the velocity references generated by these algorithms provide convergence under modeling uncertainties, but they do not imply any rule about how to keep the contact with the object. The contact can be maintained by utilizing hybrid position/force control techniques [27], [28] and/or sophisticated planning, which usually require expensive force and position sensory. Still, while applying these techniques, inaccuracies in gripper model and contact locations may result in undesired slippage or losing the contact with the object. Therefore, use of adaptive visual servoing techniques is proposed for acquiring the system model and improving the performance.

The adaptive techniques estimate a visual-motor Jacobian, which maps velocity references generated in image space to the gripper actuator space. For this purpose, [22], [29] employ an iterative Jacobian update rule based on Broyden updating formulas and a trust region method. System dynamics are also considered in [20] and [24], where an adaptive PD control rule and a neural networks based method are presented respectively. These works report faster object pose convergence, but higher oscillations in transient

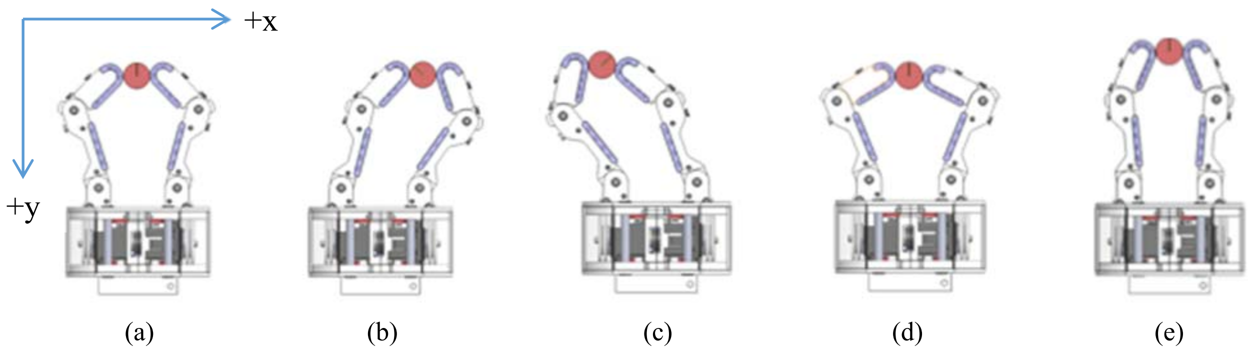

Figure 3. Manipulation with T42 hand via PMPs. PMPs are applied to the initial grasp configuration. (a) initial grasp configuration, (b) when PMP1 is applied (moving the motors in the opposite direction with the same amount), (c) when PMP2 is applied in the opposite direction, (d) when PMP2 is applied (moving the motors in the same direction with the same amount), (e) when PMP2 is applied to the opposite direction.

response. The effect of these oscillations on maintaining contact stability is unaddressed.

III. Vision-based Underactuated Precision Manipulation

The core of our approach is combining the advantages of vision feedback and adaptive underactuation using simple actuator actions called precision manipulation primitives (PMPs). These primitives provide a link by projecting the object velocity references generated by the visual servoing algorithm to the actuators space. In this way, precision manipulation is realized without any joint position feedback, force feedback or sophisticated control schemes.

The PMPs need to be designed specific to the gripper. It is assumed that an initial stable grasp is maintained a priori. We first explain the design of PMPs for the griper we used in our experiments. Following that the use of PMPs in visual servoing is covered and an adaptive extension is presented.

A. Design of PMPs for the T42 Gripper

In this paper we use Model T42 hand (Fig. 2) as an adaptive underactuated gripper. This gripper has two opposing fingers each of which have two joints and one actuator. The adaptive mechanism is obtained by the springs between the proximal and distal joints. This gripper satisfies the criteria explained in Section II.A for maintaining pinch grasp stability during manipulation: when the elastic elements are active (when the springs are not in the resting state), the fingers provide opposing force, which restores the contact with the object. The gripper also has high friction finger pads to avoid sliding. This gripper is capable of planar precision manipulation, and since it has two degrees of freedom, the object pose cannot be simultaneously controlled in all three dimensions of the planar Cartesian workspace (position in x-direction, position in y-direction, orientation around the manipulation plane), but in its 2D sub-manifold.

We use two manipulation primitives for the T42 gripper as depicted in Fig. 3:

<u>*Precision Manipulation Primitive 1:*</u> moving the actuators to opposite directions by the same increment. This primitive moves the object along the x-direction while rotating it; moving the object in negative x-direction rotates the object clockwise and vice-versa. The motion in y-direction is neglected for this primitive. These relations between the object motion and actuator velocities are expressed as follows:

$$V_{ox} = K_x \dot{q}_1 = -K_x \dot{q}_2, \tag{1}$$

$$V_{oy} = 0, \tag{2}$$

$$V_{o\theta} = -K_{\theta x} \dot{q}_1 = K_{\theta x} \dot{q}_2. \tag{3}$$

Here V_{ox} and V_{oy} are the linear velocities in x and y direction, $V_{o\theta}$ is the angular velocity around the manipulation plane normal, q_1 and q_2 are actuator positions, and K_x and $K_{\theta x}$ are scalars.

<u>*Precision Manipulation Primitive 2:*</u> moving the actuators to the same direction in the same amount. This primitive moves the object along the y-direction while rotating it. The rotation direction depends on whether the object is at the right or left side of the gripper's symmetry axis. If the object is at the right side, moving the object to the +y-direction rotates it counter-clockwise and vice versa. The amount of rotation is related to the distance of the object to the symmetry axis: No rotation is observed on the symmetry axis, and the amount of rotation increases by going further than the axis. Motion along x-direction is neglected for this primitive. These relations are expressed as follows:

$$V_{ox} = 0, \tag{4}$$

$$V_{oy} = K_y \dot{q}_1 = K_y \dot{q}_2, \tag{5}$$

$$V_{o\theta} = -p K_{\theta y} \dot{q}_1 = -p K_{\theta y} \dot{q}_2. \tag{6}$$

Here p is the distance of the symmetry axis, and K_y and $K_{\theta y}$ are a constant scalars.

These PMPs can be considered as a rough kinematics model of the manipulation process, and will be used to compose Jacobian matrices for visual servoing. PMPs are chosen to be as orthogonal as possible to span most of the manipulation workspace with few numbers of PMPs. The PMPs should be utilized so that there is always some restoration force applied by the elastic elements in order to keep the contact with the object. Assuming that such force exists in the initial grasp configuration, PMP1 preserves the restoration force by keeping the distance between actuator positions constant. While applying PMP2, $\dot{q}_1 = \dot{q}_2 > 0$ increases the restoration force while $\dot{q}_1 = \dot{q}_2 < 0$ decreases it. Therefore, a position limit should be applied for $q_1 - q_2$ for maintaining the contact.

The model generated using PMPs would not be accurate enough to conduct precise in-hand manipulation without the vision feedback; the values of K_x, K_y and K_θ changes depending on the hand and the object pose. However, coupling PMPs with the vision feedback, precision manipulation can be achieved thanks to the robustness of the visual servoing algorithms to the modeling errors. Nevertheless, more precise formulation of the PMPs can be obtained (e.g. via learning algorithms) and would help to increase the performance of the overall system.

B. Using PMPs for Visual Servoing

Generally, visual servoing schemes generate velocity references for the object using a proportional control rule:

$$V_o^{Cam} = -\lambda J_{int}^{+} e. \tag{7}$$

Here, V_o^{Cam} indicates the velocity reference for the object expressed in the camera frame, e is the feature error vector, J_{int} is the interaction matrix, J_{int}^{+} is its pseudo inverse and λ is the control gain. The resulting velocity reference needs to be transformed from camera coordinate frame to the hand coordinate frame:

$$V_o^{hand} = J_{Cam}^{hand} V_o^{Cam}. \tag{8}$$

This velocity should be projected to the actuator space. For doing that the velocity of the object in contact locations are calculated first, and transferred to the fingertip velocities:

$$V_f^{hand} = J_{contact}^{finger} J_{object}^{contact} V_o^{hand}. \tag{9}$$

Using hand Jacobian J_h, the fingertip velocities are projected to the actuated space:

$$\dot{q} = J_h V_f^{hand}. \tag{10}$$

By combining the transformations in (7)-(10), we obtain a visual-motor Jacobian J that projects feature velocities in image space to actuator velocities:

$$J = J_h J_{contact}^{finger} J_{object}^{contact} J_{cam}^{hand} J_{int}^{+}. \tag{11}$$

In this framework, PMPs replace the $J_h J_{contact}^{finger} J_{object}^{contact}$ part of the projection. As also indicated in Section III.A, the T42 hand can simultaneously control two dimensions of the three-dimensional object motion $V_o = [V_{ox}, V_{oy}, V_{o\theta}]$. By combining the PMPs expressed in (1)-(6), the following projection matrices can be obtained:

$$\begin{bmatrix}\dot{q}_1\\ \dot{q}_2\end{bmatrix} = J_{pri_{x,y}} \begin{bmatrix}V_{ox}\\ V_{oy}\end{bmatrix} = \begin{bmatrix}1/K_x & 1/K_y\\ -1/K_x & 1/K_y\end{bmatrix}\begin{bmatrix}V_{ox}\\ V_{oy}\end{bmatrix}, \tag{12}$$

$$\begin{bmatrix}\dot{q}_1\\ \dot{q}_2\end{bmatrix} = J_{pri_{x,\theta}} \begin{bmatrix}V_{ox}\\ V_{o\theta}\end{bmatrix} = \begin{bmatrix}1/K_x & -1/(pK_{\theta y})\\ -1/K_x & -1/(pK_{\theta y})\end{bmatrix}\begin{bmatrix}V_{ox}\\ V_{o\theta}\end{bmatrix}, \tag{13}$$

$$\begin{bmatrix}\dot{q}_1\\ \dot{q}_2\end{bmatrix} = J_{pri_{y,\theta}} \begin{bmatrix}V_{oy}\\ V_{o\theta}\end{bmatrix} = \begin{bmatrix}1/K_y & -1/K_{\theta x}\\ 1/K_y & 1/K_{\theta x}\end{bmatrix}\begin{bmatrix}V_{oy}\\ V_{o\theta}\end{bmatrix}, \tag{14}$$

$$\dot{q} = J_{pri} V_o^{hand}. \tag{15}$$

Object velocity expressed in the hand frame should still be transferred to the camera frame to obtain a control rule for actuators:

$$\dot{q} = -\lambda J_{pri} J_{cam}^{hand} J_{int}^{+} e. \tag{16}$$

Of course J_{pri} is a rough approximation for the $J_h J_{contact}^{finger} J_{object}^{contact}$. However, visual servoing techniques provide robustness to these inaccuracies and achieve convergence. Still, these inaccuracies affect the transient response of the system. To improve the transient response, we propose the following adaptive scheme.

C. An Adaptive Scheme

The adaptive algorithms mentioned in Section II.B estimate the visual-motor Jacobian, (J matrix in (11)) by iteratively minimizing the difference between the calculated and measured feature locations. These methods may lead to the loss of contact with the object while exploring the parameter space, inaccuracies during the transient of the adaptation result in projecting actuator velocities different than the desired values. Moreover, within the framework of this paper, such adaptation cannot be employed since it bypasses the projection via PMPs, and directly transfers the velocity to the actuator space.

Instead, we propose to calculate a projection matrix that maps the unit vector of current object velocity to the unit vector of desired velocities:

$$\bar{V}_o^{hand^*} = H \bar{V}_o^{hand^{cur}}. \tag{17}$$

In this equation $\bar{V}_o^{hand^*}$ and $\bar{V}_o^{hand^{cur}}$ signifies desired and current unit vectors in hand coordinate frame respectively. In this formulation, it is preferred to calculate the projection between the unit vectors rather than the vectors with magnitudes in order to avoid velocity fluctuations and achieve smoother motions during the transient of the adaptation.

The unit vectors can be calculated by using desired and current image trajectories:

$$\bar{V}_o^{hand^*} = J_{cam}^{hand} J_{int}^{+} v_{f_d} / \left| J_{cam}^{hand} J_{int}^{+} v_{f_d} \right|, \tag{18}$$

$$\bar{V}_o^{hand^{cur}} = J_{cam}^{hand} J_{int}^{+} v_f / \left| J_{cam}^{hand} J_{int}^{+} v_f \right|. \tag{19}$$

where v_f and v_{f_d} are current and desired feature velocity vectors respectively. The H matrix can then be used as a correction term in the projection.

$$\dot{q} = -\lambda J_{pri} H J_{cam}^{hand} J_{int}^{+} e. \tag{20}$$

IV. Experimental Results:

The performance of the proposed vision-based control scheme was evaluated with planar manipulation experiments using the T42 gripper. The experimental setup can be seen in Fig. 4. The frame rate of the camera was 30 fps, the image resolution was 640x480 pixels and the distance between the camera and the object top plane was 18.5cm. For analyzing the effect of object's shape and size on systems performance, we used rectangles and cylinders in three different sizes (Fig. 5). We placed markers (a point and a line) on the objects to indicate the center point of their top surfaces and their direction.

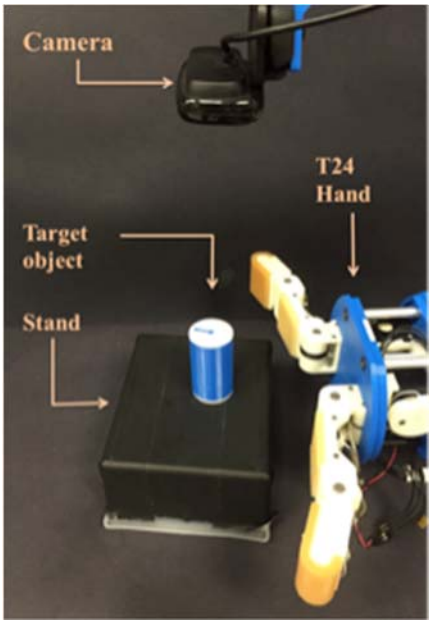

Figure 4. Experimental Setup.

Prior to precision manipulation, the target object is placed on a stand and pinch-grasped around its center. Then, the stand is removed and the object is manipulated by the gripper without the plane support.

Three sets of experiments are conducted to analyze various aspects of the proposed method. In the first set, the regulation performance of the system is tested with varying object sizes and shapes. In the second set, the tracking performance of the method is evaluated with linear and circular references in several parts of the workspace. In the third set, results with the adaptive method is presented and compared with the non-adaptive case.

A. Regulation Experiments:

As explained in Section III, the T42 gripper can simultaneously control the object pose in two dimensions of the 3 dimensional Cartesian space. For controlling the position of the object in x and y-directions, projection in eq. 12 is used (case 1), for positioning in x-direction while controlling the orientation of the object, the projection in eq. 13 (case 2) is used, and for positioning in y-direction while controlling the orientation, the projection in eq. 14 (case 3) is used.

Figure 5. Objects used in the experiments. Cylinders with 2, 3 and 4 cm diameters, and rectangular prisms with dimensions 2x4, 3x5 and 4x6 cm. 0.5 cm thick rubber clothing is used with prisms to increase the contact friction. The objects' weights vary between 12 g and 75 g.

For case 1, the set points (SPs) in Fig. 6a are used. The system is initialized at SP 1, and the set points 2-10 are applied sequentially; when the error remains less than 3 pixels for 1 second, next SP is applied. These experiments are conducted with all the objects in Fig. 5.

In the experiments, all the set points are successfully reached with all the cylindrical objects. For the middle size cylinder, snapshots are given in Fig. 7 as the set points are reached, and the trajectory of the object is presented in Fig. 8. It is observed that the system follows a path that is close to ideal, when the Jacobian obtained using the PMPs is closer to the real projection. However, close to the edges of the workspace (SPs 8, 9 and 10), the inaccuracy in the Jacobian matrix causes divergence from the ideal path. Still, vision feedback provides enough robustness to maintain the convergence. For small, medium and large cylinders the total travel distance in pixels 734, 669 and 605, which took 110, 93 and 90 seconds respectively. We can see a trend that, as the size of the cylinder increases the system's performance gets better.

The SPs could not be realized with any of the rectangular objects. The reason was that, the rectangles flip within the hand, and the contact points shift to the corners of the object (Fig. 9). This phenomenon happens at the edges of the workspace, and results in losing the object. This is also valid for cases 2 and 3.

For case 2, the experiments are conducted with the medium size cylinder. The green lines in Fig. 6b are used as

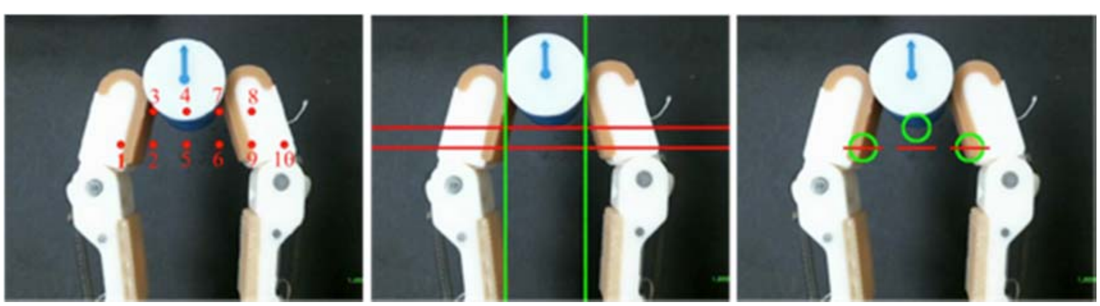

Figure 6. References used in the experiments. (a) 10 set points for regulation experiments, (b) x references (green lines) and y references (red lines) for experiments with orientation manipulation. (c) references for tracking experiments: Circle and line references.

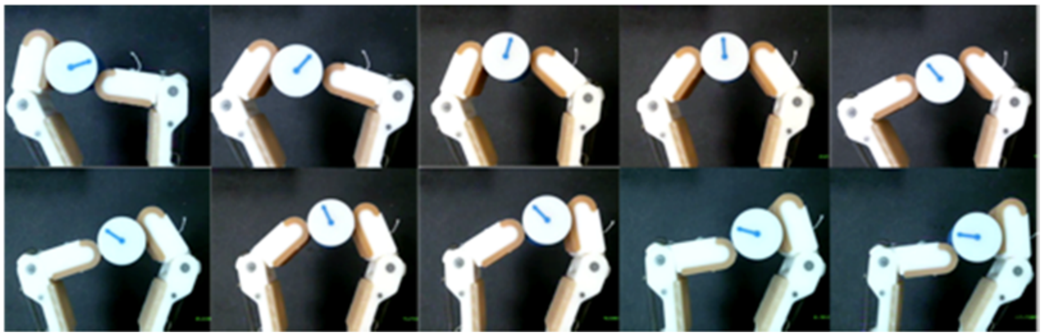

Figure 7. The poses of the hand-object couple during the regulation experiment using the middle size cylinder. Top line: when the object is on SP 1-5; Bottom line: when the object is on SP 6-10.

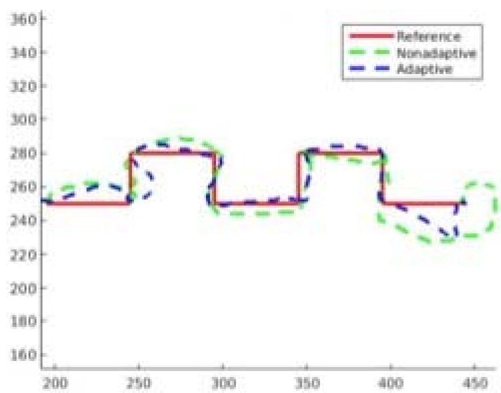

Figure 8. Regulation experiments.

Figure 9. Failure mode with a rectangular object.

x position references, while orientation references are set to +45 and +60 for the left line and -45 and -60 for the right line. All references are met successfully and settling times are measured as 10.4, 23.8, 17.4 and 26.3 seconds respectively.

For case 3, red lines in Fig. 6b are used for y position references, and orientation references are given as +45, -45 for both lines. Again, all the references are successfully met, and the settling times for the upper line are measured as 8.9, and 7.2, whereas the values for the lower line are measured as 17.6, and 18.7 seconds.

B. Tracking Experiments

The tracking performance of the system is evaluated with line and circle references. For the linear reference, a sine signal with amplitude 60 is applied as a reference in x-direction. For the circular reference two sine signals with amplitude 20 is applied to x and y-direction with 90 degrees phase shift. The frequency of the sine signals is 0.25 Hz. These periodic signals are applied in three different positions of the workspace as can be seen in Fig. 6c. As target object medium size cylinder and rectangular objects are used. The results are summarized in Table I.

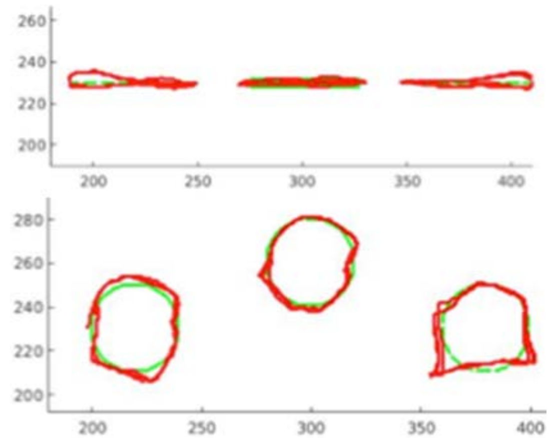

Figure 10. Tracking results. Green: reference signal, red: trajectory of the target feature.

For rectangular prisms, only the central circle can be tracked, since the failure mode in Fig. 9 occurs at the side circles. The results with the prisms show worse tracking performance than the cylinders, which is due to high within-hand rotation of the prisms during manipulation. For medium size cylinder, it can be seen both in Table I and Fig. 10 that the tracking performance is better at the center of the workspace. These results are also consistent with the regulation experiments.

C. Adaptive Method Experiments

The effectiveness of the proposed adaptive method is tested with the regulation experiment in Section IV.A which uses the SPs in Fig. 6.a. The medium size cylinder is used as the target object. Three regulation experiment are conducted both for the adaptive and non-adaptive case. The trajectories of one of the trials are presented in Fig. 8. It is seen that the adaptive method is especially effective when the deviation from the optimal path is large which happens at the edges of the workspace. The average time of the three trials with the adaptive method is 63.8 seconds, where as it is 81.4 for the non-adaptive case. Also average pixel travel for the three trials results in 540.2 pixels for the adaptive case, and 672.3 for the non-adaptive method. These results show that the proposed adaptive extension is effective for improving the transient performance of the system.

TABLE I. AVERAGE AND MAXIMUM ERROR FOR TRACKING EXPERIMENTS IN PIXELS. RESULTS WITH RECTANGULAR OBJECTS AND MEDIUM SIZE CYLINDER.

		Ave. err.	Max. err. x-dir.	Max. err. y-dir.
M. Cylinder	Left Line	3.5	11	6
	Center Line	2.6	8	3
	Right Line	3.8	10	5
	Left Circle	4.5	4	13
	Center Circle	3.2	2	2
	Right Circle	4.6	7	9
S. Rec. Cen. Circ.		4.4	9	19
M. Rec. Cen. Circ.		5.6	15	21
L. Rec. Cen. Circ.		4.7	16	20

V. CONCLUSIONS

In this paper, we proposed the use of precision manipulation primitives for enabling vision-based dexterous manipulation with underactuated grippers. The primitives are used as a link that projects the velocity commands of the visual servoing algorithm to the actuators while keeping the contact restoration force active. It is seen that, with such a scheme, reliable vision-based precision manipulation can be conducted, and its performance can further be improved with an adaptive approach. We believe that the proposed method can also be applied to fully-actuated grippers if the role of the elastic elements of underactuated hands can be mimicked using an impedance control technique.

As a future work, we plan to assess the performance of the algorithm with a larger variety of object shapes and grippers. We also aim to employ an iterative learning control in the visual servoing rule for improving the performance of the system while tracking periodic signals. Furthermore, we will focus on detecting the manipulation workspace limits online by observing the pose of the fingers and the object within hand. By this way, we plan to avoid workspace limits by utilizing online path planning algorithms.

REFERENCES

[1] I. M. Bullock, R. R. Ma, and A. M. Dollar, "A hand-centric classification of human and robot dexterous manipulation.," *IEEE Trans. Haptics*, vol. 6, no. 2, pp. 129–44, Jan. 2013.

[2] R. R. Ma and A. M. Dollar, "On dexterity and dexterous manipulation," *IEEE 15th Int. Conf. Adv. Robot. New Boundaries Robot. ICAR 2011*, pp. 1–7, 2011.

[3] A. Bicchi, C. Melchiorri, and D. Balluchi, "On the mobility and manipulability of general multiple limb robots," *IEEE Trans. Robot. Autom.*, vol. 11, no. 2, pp. 215–228, 1995.

[4] Y. Li and I. Kao, "A review of modeling of soft-contact fingers and stiffness control for dextrous manipulation in robotics," *Proc. 2001 ICRA. IEEE Int. Conf. Robot. Autom. (Cat. No.01CH37164)*, vol. 3, pp. 3055–3060, 2001.

[5] R. Michalec and A. Micaelli, "Stiffness modeling for multi-fingered grasping with rolling contacts," *2010 10th IEEE-RAS Int. Conf. Humanoid Robot. Humanoids 2010*, pp. 601–608, 2010.

[6] T. Yamada, T. Taki, M. Yamada, and H. Yamamoto, "Static Grasp Stability Analysis of Two Spatial Objects Including Contact Surface Geometry," *Trans. Control Mech. Syst.*, vol. 25, pp. 218–228, 2012.

[7] A. M. Okamura, N. Smaby, and M. R. Cutkosky, "An overview of dexterous manipulation," *Proc. 2000 ICRA. Millenn. Conf. IEEE Int. Conf. Robot. Autom. Symp. Proc. (Cat. No.00CH37065)*, vol. 1, no. April, 2000.

[8] L. U. Odhner, L. P. Jentoft, M. R. Claffee, N. Corson, Y. Tenzer, R. R. Ma, M. Buehler, R. Kohout, R. D. Howe, and A. M. Dollar, "A compliant, underactuated hand for robust manipulation," *Int. J. Rob. Res.*, vol. 33, no. 5, pp. 736–752, 2014.

[9] R. Deimel and O. Brock, "A novel type of compliant and underactuated robotic hand for dexterous grasping," *Int. J. Rob. Res.*, vol. 35, no. 1–3, pp. 161–185, 2016.

[10] L. U. Odhner and A. M. Dollar, "Dexterous manipulation with underactuated elastic hands," in *2011 IEEE International Conference on Robotics and Automation*, 2011, pp. 5254–5260.

[11] L. U. Odhner and A. M. Dollar, "Stable, open-loop precision manipulation with underactuated hands," *Int. J. Rob. Res.*, vol. 34, no. 11, pp. 1347–1360, 2015.

[12] D. Prattichizzo, M. Malvezzi, M. Gabiccini, and A. Bicchi, "On the manipulability ellipsoids of underactuated robotic hands with compliance," *Rob. Auton. Syst.*, vol. 60, pp. 337–346, 2012.

[13] L. U. Odhner, R. R. Ma, and A. M. Dollar, "Experiments in Underactuated In-Hand Manipulation," *Exp. Robot.*, vol. 88, pp. 27–40, 2013.

[14] R. R. Ma, N. Rojas, and A. M. Dollar, "Towards predictable precision manipulation of unknown objects with underactuated fingers," *Mech. Mach. Sci.*, vol. 36, pp. 927–937, 2016.

[15] J. Borras and A. M. Dollar, "A parallel robots framework to study precision grasping and dexterous manipulation," *Proc. IEEE Int. Conf. Robot. Autom.*, pp. 1595–1601, 2013.

[16] S. Darma, J. L. Buessler, G. Hermann, J. P. Urban, and B. Kusumoputro, "Visual servoing quadrotor control in autonomous target search," *Proc. 2013 IEEE 3rd Int. Conf. Syst. Eng. Technol. ICSET 2013*, pp. 319–324, 2013.

[17] K. Wang, Y. Liu, and L. Li, "Visual servoing trajectory tracking of nonholonomic mobile robots without direct position measurement," *IEEE Trans. Robot.*, vol. 30, no. 4, pp. 1026–1035, 2014.

[18] G. P. Moustris, S. C. Hiridis, K. M. Deliparaschos, and K. M. Konstantinidis, "Evolution of autnomous and semi-autnomous robotic surgical systems: a review of the literature," *Int. J. Med. Robot.*, vol. 7, no. August 2013, pp. 375–392, 2011.

[19] P. K. Allen, A. T. Miller, P. Y. Oh, and B. S. Leibowitz, "Using tactile and visual sensing with a robotic hand," *Proc. Int. Conf. Robot. Autom.*, vol. 1, pp. 676–681, 1997.

[20] C. C. Cheah, H. Y. Han, S. Kawamura, and S. Arimoto, "Grasping and Position Control for Multi-fingered Robot Hands with Uncertain Jacobian Matrices," in *Proceedings of the 1998 IEEE International Conference on Robotics & Automation*, 1998, pp. 2403–2408.

[21] M. Jägersand, O. Fuentes, and R. Nelson, "Acquiring visual-motor models for precision manipulation with robot hands," in *Computer Vision—ECCV'96*, 1996, no. 1, pp. 603–612.

[22] M. Jagersand, O. Fuentes, and R. Nelson, "Experimental evaluation of uncalibrated visual servoing for precision manipulation," *Proc. Int. Conf. Robot. Autom.*, vol. 4, 1997.

[23] C. A. Jara, J. Pomares, F. A. Candelas, F. Torres, and S. Member, "Optimal control for robot - hand manipulation of an object using dynamic visual servoing," *Iros*, no. Iros, 2014.

[24] Y. Zhao and C. C. Cheah, "Neural network control of multifingered robot hands using visual feedback.," *IEEE Trans. neural networks*, vol. 20, no. 5, pp. 758–67, 2009.

[25] L. A. Munoz, "Robust dexterous manipulation: a methodology using visual servoing," *Proceedings. 1998 IEEE/RSJ Int. Conf. Intell. Robot. Syst. Innov. Theory, Pract. Appl. (Cat. No.98CH36190)*, vol. 1, no. October, pp. 292–297, 1998.

[26] F. Chaumette and S. Hutchinson, "Visual servo control. I. Basic approaches," *IEEE Robot. Autom. Mag.*, vol. 13, no. 4, pp. 82–90, 2006.

[27] K. Hosoda, K. Igarashi, and M. Asada, "Adaptive hybrid visual servoing/force control in unknownenvironment," *Proc. IEEE/RSJ Int. Conf. Intell. Robot. Syst. IROS '96*, vol. 3, pp. 1097–1103, 1996.

[28] N. Vahrenkamp, C. Böge, K. Welke, T. Asfour, J. Walter, and R. Dillmann, "Visual servoing for dual arm motions on a humanoid robot," *9th IEEE-RAS Int. Conf. Humanoid Robot. HUMANOIDS09*, pp. 208–214, 2009.

[29] M. Jägersand, "Visual servoing using trust region methods and estimation of the full coupled visual-motor jacobian," *Image (IN).*, vol. 11, p. 1, 1996.